

NEUROSYSTEMS

Subthalamo-pallidal interactions underlying parkinsonian neuronal oscillations in the primate basal ganglia

Yoshihisa Tachibana,^{1,2} Hirokazu Iwamuro,¹ Hitoshi Kita,³ Masahiko Takada⁴ and Atsushi Nambu^{1,2}¹Division of System Neurophysiology, National Institute for Physiological Sciences, Okazaki, Aichi, Japan²Department of Physiological Sciences, The Graduate University for Advanced Studies, Okazaki, Aichi, Japan³Department of Anatomy and Neurobiology, College of Medicine, University of Tennessee Health Science Center, Memphis, TN, USA⁴Systems Neuroscience Section, Primate Research Institute, Kyoto University, Inuyama, Aichi, Japan**Keywords:** GABA, globus pallidus, glutamate, parkinsonian monkeys, subthalamic nucleus

Abstract

Parkinson's disease is characterized by degeneration of nigral dopaminergic neurons, leading to a wide variety of psychomotor dysfunctions. Accumulated evidence suggests that abnormally synchronized oscillations in the basal ganglia contribute to the expression of parkinsonian motor symptoms. However, the mechanism that generates abnormal oscillations in a dopamine-depleted state remains poorly understood. We addressed this question by examining basal ganglia neuronal activity in two 1-methyl-4-phenyl-1,2,3,6-tetrahydropyridine-treated parkinsonian monkeys. We found that systemic administration of L-3,4-dihydroxyphenylalanine (L-DOPA; dopamine precursor) decreased abnormal neuronal oscillations (8–15 Hz) in the internal segment of the globus pallidus (GPi) and the subthalamic nucleus (STN) during the ON state when parkinsonian signs were alleviated and during L-DOPA-induced dyskinesia. GPi oscillations and parkinsonian signs were suppressed by silencing of the STN with infusion of muscimol (GABA_A receptor agonist). Intrapallidal microinjection of a mixture of 3-(2-carboxypiperazin-4-yl)-propyl-1-phosphonic acid (CPP; N-methyl-D-aspartate receptor antagonist) and 1,2,3,4-tetrahydro-6-nitro-2,3-dioxo-benzo[*f*]quinoxaline-7-sulfonamide (NBQX; AMPA/kainate receptor antagonist) also decreased the oscillations in the GPi and the external segment of the globus pallidus (GPe). Neuronal oscillations in the STN were suppressed after intrasubthalamic microinjection of CPP/NBQX to block glutamatergic afferents of the STN. The STN oscillations were further reduced by muscimol inactivation of the GPe to block GABAergic inputs from the GPe. These results suggest that, in the dopamine-depleted state, glutamatergic inputs to the STN and reciprocal GPe–STN interconnections are both important for the generation and amplification of the oscillatory activity of STN neurons, which is subsequently transmitted to the GPi, thus contributing to the symptomatic expression of Parkinson's disease.

Introduction

Degeneration of nigral dopaminergic neurons is associated with motor symptoms of Parkinson's disease (PD), which include bradykinesia, rigidity, and tremor. Changes in the firing rates of basal ganglia (BG) neurons are thought to induce the PD symptoms (Albin *et al.*, 1989; DeLong, 1990). Contrary to the rate-based theory, the pathophysiology of PD is often correlated with abnormal burst firing and oscillatory activity in the BG (Filion, 1979; Wichmann *et al.*, 1994; for reviews, see Boraud *et al.*, 2002; Brown, 2003; Gatev *et al.*, 2006; Rivlin-Etzion *et al.*, 2006a; Hammond *et al.*, 2007). Single/multi-unit activity and local field potentials (LFPs) recorded from parkinsonian animals and patients have shown that oscillatory activity and neuronal synchronization in the globus pallidus and the subthalamic nucleus

(STN) include two major frequency bands: the 'tremor-related' 3–8-Hz band and the higher 8–30-Hz band (Bergman *et al.*, 1994; Levy *et al.*, 2000; Brown *et al.*, 2001). However, the mechanisms regulating the abnormal BG oscillations remain unknown.

The first goal of the present study was to examine whether parkinsonian BG oscillations might depend on dopaminergic inputs. Dopamine therapy can ameliorate parkinsonian signs and, at least partly, reverse the abnormal firing pattern of spike trains (Boraud *et al.*, 1998; Levy *et al.*, 2001a, 2002; Heimer *et al.*, 2006; Lafreniere-Roula *et al.*, 2010) and neuronal synchronization observed in LFPs (Brown *et al.*, 2001; Cassidy *et al.*, 2002; Priori *et al.*, 2004) in the BG. However, little is known about systemic dopamine-dependent changes in the firing properties of neurons of the internal segment of the globus pallidus (GPi), external segment of the globus pallidus (GPe) and STN in the same parkinsonian subject. Thus, we tested the effects of intravenous L-3,4-dihydroxyphenylalanine (L-DOPA) injection on BG neuronal activity in 1-methyl-4-phenyl-1,2,3,6-tetrahydropyridine (MPTP)-treated monkeys (Fig. 1A). The second

Correspondence: Atsushi Nambu and Yoshihisa Tachibana, ¹Division of System Neurophysiology, as above.

E-mails: nambu@nips.ac.jp and banao@nips.ac.jp

Received 20 May 2011, revised 3 August 2011, accepted 8 August 2011

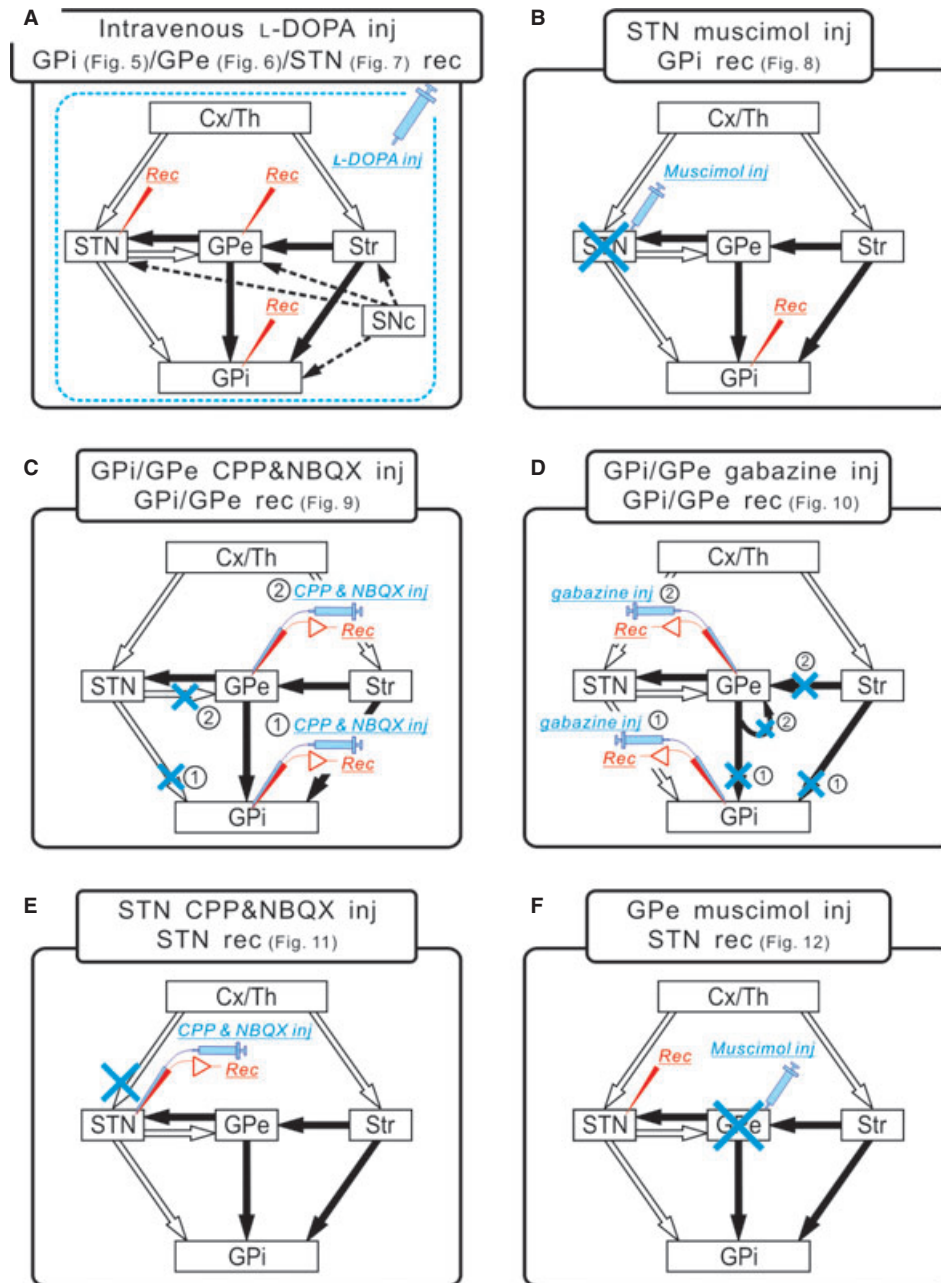


FIG. 1. Schematic diagrams of experiments in parkinsonian monkeys. Anatomical connections within cortico-BG circuits are shown. Open, filled and broken arrows represent glutamatergic, GABAergic and dopaminergic projections, respectively. The striatum (Str) and STN are two major input nuclei of the BG. Inputs from the cortex (Cx) and the thalamus (Th) enter the two nuclei and finally reach the GPI, an output nucleus of the BG. The GPe is positioned as an intermediate relay system, which is reciprocally interconnected with the STN. Dopaminergic projections from the substantia nigra pars compacta (SNc) are widely distributed in the BG. The following experiments were performed to examine the mechanisms regulating abnormal neuronal oscillations in the BG. (A) Single-unit recording of a GPI, a GPe or an STN neuron with intravenous injection of the dopamine precursor L-DOPA to restore dopamine levels (see Fig. 5 for GPI, Fig. 6 for GPe, and Fig. 7 for STN). (B) Recording from a GPI neuron with muscimol injection into the STN to block subthalamic inputs to the GPI (see Fig. 8). (C) Recording from a GPI (1) or a GPe (2) neuron with intrapallidal microinjection of the ionotropic glutamate receptor antagonists CPP and NBQX to block glutamatergic inputs to the GPI or GPe (see Fig. 9A–G for GPI and Fig. 9H–N for GPe). (D) Recording from a GPI (1) or a GPe (2) neuron with intrapallidal microinjection of the ionotropic GABA receptor antagonist gabazine to block GABAergic inputs to the GPI or GPe (see Fig. 10). Gabazine injection into the GPI blocked GABAergic inputs from the Str and GPe, and injection into the GPe blocked the inputs from the Str and GPe axon collaterals. (E) Recording from an STN neuron with intrasubthalamic microinjection of CPP and NBQX to block glutamatergic inputs to the STN (see Fig. 11). (F) Recording from an STN neuron with muscimol injection into the GPe to block GPe-derived GABAergic inputs (see Fig. 12).

goal of our study was to clarify the origin of GPI/GPe oscillations. Recordings of LFPs from PD patients show elevated levels of coherence between the STN and GPI (Brown *et al.*, 2001). The STN consists of glutamatergic projection neurons, and strongly influences GPI/GPe activity. To provide direct evidence that STN oscillations

may drive oscillations in the GPI/GPe, we performed single-unit GPI/GPe recordings while STN glutamatergic inputs were blocked (Fig. 1B and C). Finally, the origin of STN oscillations was also investigated. Glutamatergic inputs from the cerebral cortex and the thalamus may drive STN oscillations (Magill *et al.*, 2000, 2001;

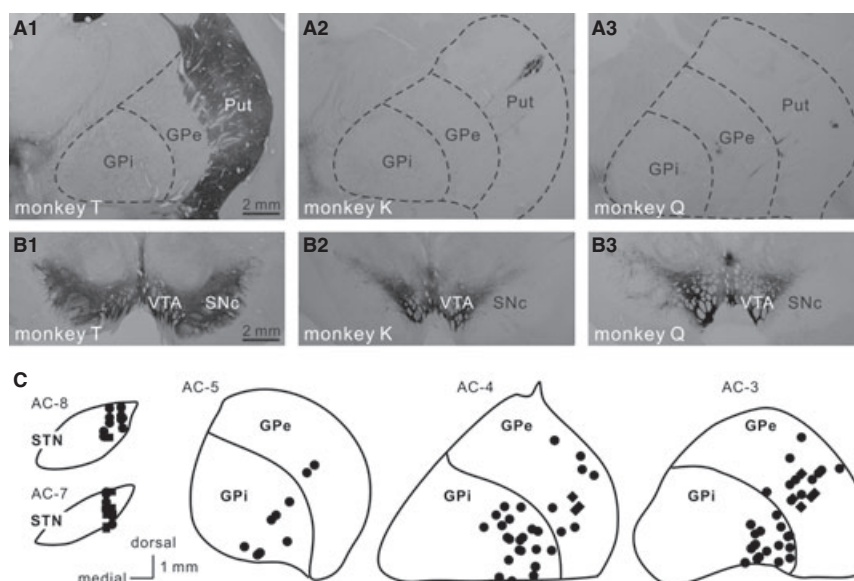


FIG. 2. TH immunoreactivity in the BG sampled from normal and MPTP-treated monkeys, and sites of unit recordings and drug injections in the STN and GPi/GPe. (A and B) Photomicrographs showing TH immunoreactivity in the putamen (Put; A1–A3) and the midbrain tegmentum (B1–B3). Sections in A1 and B1 are from a normal monkey (monkey T), and sections in A2, A3, B2 and B3 are from MPTP-treated monkeys (monkeys K and Q). As compared with the control (A1 and B1), marked reductions in TH immunoreactivity were observed in the Put (A2 and A3) and the ventral tier of the substantia nigra pars compacta (SNc) (B2 and B3) of the MPTP-treated monkeys. Note that numbers of TH-positive cells still remain in the dorsal tier of the SNc and the ventral tegmental area (VTA). The sections shown in A2 and A3 and the right side of the sections shown in B2 and B3 represent the sides ipsilateral to the carotid injections of MPTP and electrophysiological recordings. (C) Sites of unit recordings and drug injections in the STN and GPi/GPe are reconstructed from two MPTP-treated monkeys, and superimposed on representative coronal sections. Levels of the sections are indicated as distances (mm) from the caudal end of the anterior commissure (AC). Filled circles and squares represent the recording and injection sites, respectively. These sites are located within the motor territories of the STN and GPi/GPe (Nambu *et al.*, 2000; Tachibana *et al.*, 2008).

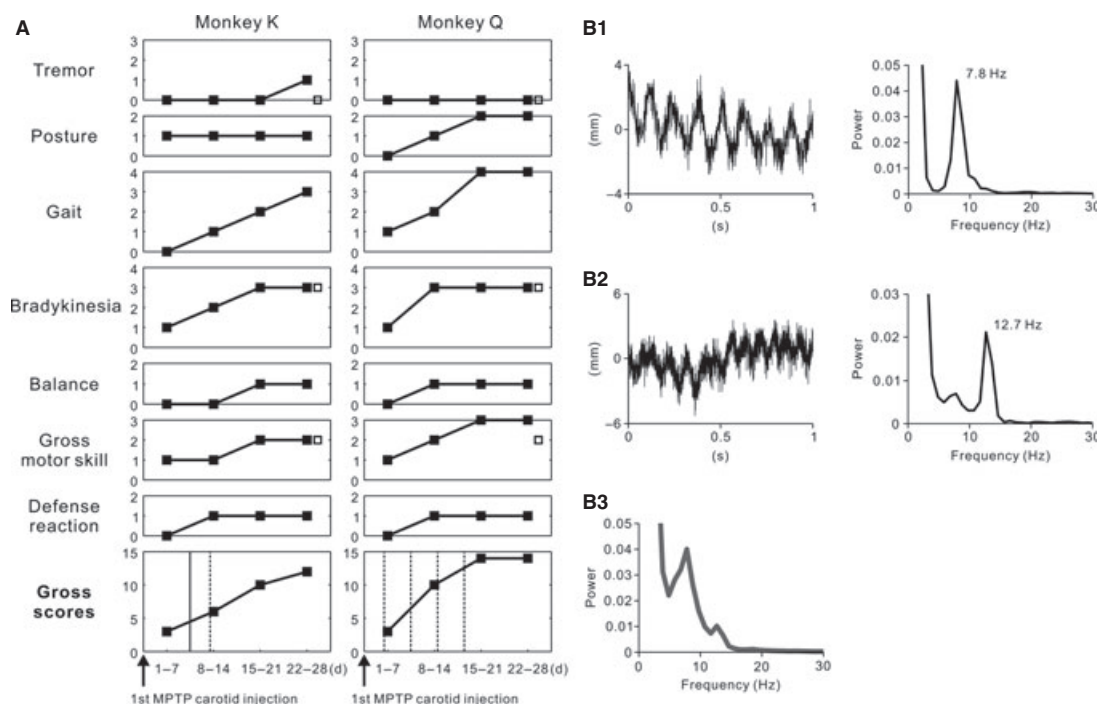


FIG. 3. Parkinsonian motor signs. (A) Parkinsonian rating scale. With the monkey parkinsonian rating scale of Smith *et al.* (1993), a variety of motor signs were evaluated (see also Supporting Information Data S1). Partial and gross motor scores are plotted along the time course (days) after the first carotid injection of MPTP. Filled and open squares represent the scores on the contralateral or ipsilateral side to the carotid injection, respectively. The partial scores on the ipsilateral side were estimated only at the behaviorally stable stage. The solid vertical line for the gross scores represents the timing of the second MPTP carotid injection. The broken vertical lines represent the timings of additional intravenous MPTP injections. (B) Resting tremor in monkey K. Small forearm movements were detected with a laser displacement sensor (LK-500; sampling rate, 1 kHz; Keyence, Osaka, Japan). (B1 and B2) Two representative raw data of a 7.8-Hz dominant (B1) and a 12.7-Hz dominant (B2) tremor episode are shown in the left panels. The power spectra of each tremor episode are shown in the right panels. Power spectrum analyses were performed with 5-s raw data with a non-overlapping Hann window of 1024 bins, yielding a spectral resolution of 1 Hz. (B3) Averaged power spectrum from 41 tremor episodes, exhibiting two peaks at 7.8 and 12.7 Hz.

TABLE 1. Electrophysiological properties of GPe, GPi and STN neurons recorded before and after MPTP injections. (A) Monkey K. (B) Monkey Q

	GPe		GPi		STN	
	Normal (<i>n</i> = 51)	MPTP (<i>n</i> = 41)	Normal (<i>n</i> = 52)	MPTP (<i>n</i> = 32)	Normal (<i>n</i> = 47)	MPTP (<i>n</i> = 30)
(A)						
Firing rate (Hz)	64.7 ± 27.5	44.7 ± 23.1**	70.3 ± 26.0	73.0 ± 30.4	20.8 ± 11.4	30.7 ± 13.0***
Percentage of spikes in bursts (%)	14.0 ± 12.8	23.1 ± 17.2**	10.6 ± 11.3	22.7 ± 17.4***	24.4 ± 12.9	36.2 ± 12.0***
Mean 'surprise value'	4.30 ± 1.13	4.99 ± 2.11	4.32 ± 0.89	5.22 ± 2.33**	5.55 ± 1.50	5.71 ± 1.14
Number of 3–8-Hz oscillatory cells (%)	9/51 (17.6)	4/41 (9.8)	25/52 (48.1)	12/32 (37.5)	4/47 (8.5)	4/30 (6.7)
Mean 3–8-Hz power	1.09 ± 0.14	1.06 ± 0.12	1.26 ± 0.30	1.22 ± 0.43	1.04 ± 0.10	1.10 ± 0.13
Number of 8–15-Hz oscillatory cells (%)	0/51 (0.0)	4/41 (9.8)*	0/52 (0.0)	23/32 (71.9)***	4/47 (8.5)	10/30 (33.3)**
Mean frequency with maximum power at 8–15 Hz (Hz)	NA	12.6 ± 1.3 (<i>n</i> = 4)	NA	12.7 ± 1.3 (<i>n</i> = 23)	11.0 ± 2.2 (<i>n</i> = 4)	13.5 ± 0.6 (<i>n</i> = 10)
Mean 8–15-Hz power	0.82 ± 0.10	0.95 ± 0.13***	0.87 ± 0.10	1.31 ± 0.29***	0.97 ± 0.10	1.10 ± 0.13***
(B)						
Firing rate (Hz)	65.6 ± 24.2	37.6 ± 21.6***	64.8 ± 22.9	58.4 ± 23.9	18.6 ± 7.6	23.9 ± 8.0*
Percentage of spikes in bursts (%)	14.7 ± 14.4	41.1 ± 24.1***	7.0 ± 7.0	20.2 ± 15.0***	32.6 ± 16.4	40.9 ± 14.9*
Mean 'surprise value'	4.53 ± 1.25	6.73 ± 3.15***	4.13 ± 0.97	4.98 ± 1.40**	5.36 ± 1.24	6.14 ± 1.72*
Number of 3–8-Hz oscillatory cells (%)	17/54 (31.5)	11/40 (27.5)	28/75 (37.3)	28/68 (41.2)	1/44 (2.2)	4/25 (16.0)*
Mean 3–8-Hz power	1.13 ± 0.24	1.18 ± 0.17	1.15 ± 0.25	1.18 ± 0.28	1.00 ± 0.19	1.13 ± 0.20**
Number of 8–15-Hz oscillatory cells (%)	0/54 (0.0)	4/40 (10.0)*	0/75 (0.0)	23/68 (33.8)***	2/44 (4.5)	6/25 (24.0)*
Mean frequency with maximum power at 8–15 Hz (Hz)	NA	10.7 ± 0.8 (<i>n</i> = 4)	NA	11.4 ± 1.0 (<i>n</i> = 23)	11.7 ± 3.5 (<i>n</i> = 2)	10.7 ± 1.9 (<i>n</i> = 6)
Mean 8–15-Hz power	0.79 ± 0.13	0.87 ± 0.13*	0.76 ± 0.11	1.05 ± 0.36***	0.94 ± 0.17	1.02 ± 0.15*

Firing properties of GPe, GPi and STN neurons are represented as mean ± SD. Mann–Whitney *U*-tests were performed between normal and parkinsonian states. The proportions of oscillatory cells were compared by use of Fisher's exact tests. NA, data not available. Significance levels are as follows: **P* < 0.05, ***P* < 0.01, ****P* < 0.001.

Williams *et al.*, 2002; Sharott *et al.*, 2005; Mallet *et al.*, 2008b). It has also been demonstrated by Baufreton *et al.* (2005a) that excitation together with feedback GABAergic inhibition from the GPe is sufficient to generate highly synchronous activity (15–30 Hz) of STN neurons *in vitro*. However, it is unknown how the glutamatergic and pallidal GABAergic inputs contribute to STN oscillations. To address this issue, we examined STN activity during blockade of the two synaptic inputs (Fig. 1E and F). We found that, in the dopamine-depleted state, the oscillatory activity of STN neurons is generated by both the glutamatergic and the GPe-derived GABAergic inputs, and finally transmitted to the GPi.

Materials and methods

Surgical procedures

Two male monkeys (*Macaca cyclopis*, monkey K, and *Macaca mulatta*, monkey Q) weighing 3.5–5.0 kg were used as subjects in this study. The experimental protocols were approved by the Institutional Animal Care and Use Committee of National Institutes of Natural Sciences, and all experiments were conducted according to the guidelines of the National Institutes of Health *Guide for the Care and Use of Laboratory Animals*.

Prior to the experiments, each monkey was trained to sit quietly in a monkey chair. Under general anesthesia with intramuscular ketamine hydrochloride (10 mg/kg body weight) and intravenous sodium pentobarbital (25 mg/kg), the monkeys underwent a surgical procedure for head fixation and extracellular recordings of GPi/GPe and STN neurons, as reported previously (Nambu *et al.*, 2000; Tachibana *et al.*, 2008). Magnetic resonance imaging (3T Allegra; Siemens, Erlangen, Germany) scans were performed to estimate stereotaxic coordinates of the brain structures. Recordings of neuronal activity in the GPi/GPe and STN under normal conditions were initiated 2 weeks after the initial surgery.

Electrophysiological recording

During the recording sessions, each monkey was in an awake state and seated in the monkey chair with his head restrained. Single-unit recordings of GPi/GPe and STN neurons were performed with a glass-coated Elgiloy microelectrode (0.8–1.2 M Ω at 1 kHz for GPi/GPe; 1.5–2.0 M Ω for STN). The electrode was inserted obliquely (45° from vertical in the frontal plane) into the GPi/GPe or vertically into the STN with a hydraulic microdrive. The unitary activity recorded from the microelectrode was amplified ($\times 8000$), filtered (100 Hz to 2 kHz), converted into digital data with a window discriminator, and sampled at 2 kHz with a computer. In this study, we examined neuronal populations sampled from the motor territories (forelimb and orofacial regions) of the GPi/GPe and STN (Nambu *et al.*, 2000; Tachibana *et al.*, 2008); the recording sites were located in the lateral parts of individual structures at their middle to caudal levels (Fig. 2C). The subdivisions of the pallidum (i.e. GPe and GPi) were determined by the depth of recording electrodes, firing patterns and decreased electrical signals in the lamina between the GPe and GPi (Nambu *et al.*, 2000). The monkey's arousal level was visually monitored and maintained during recording sessions. Only stable and well-isolated neurons were included in the present data.

MPTP injections

After the recordings of GPi/GPe and STN neurons in the normal state, systemic administration of MPTP (Sigma, St Louis, MO, USA) was

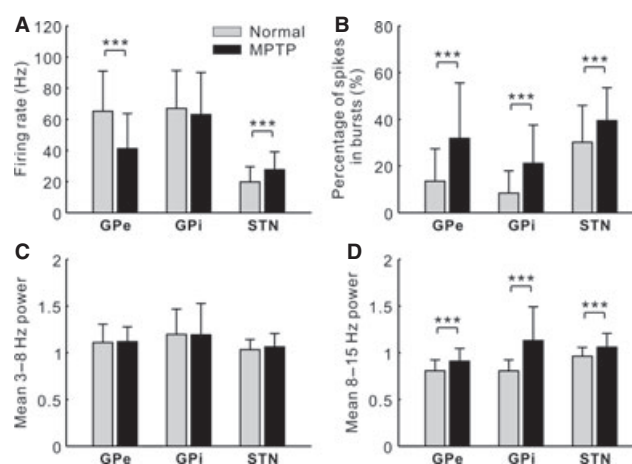


FIG. 4. Comparison of electrophysiological properties of BG neurons in normal and parkinsonian monkeys. (A) Spontaneous firing rates. Gray and black columns show the average firing rates in normal and MPTP-treated monkeys, respectively. Data are given as mean \pm SD. The same conventions are used in B–D. The GPe firing rate was significantly decreased after MPTP treatment, whereas the STN firing rate was significantly increased. (B) Percentage of spikes in bursts. The bursts were detected with the 'Poisson surprise' algorithm. The burst strength was increased in all three structures. (C) Averaged power of 3–8-Hz oscillatory activity. Oscillatory activity was calculated on the basis of the algorithm of Rivlin-Etzion *et al.* (2006b). There were no changes in 3–8-Hz oscillatory activity. (D) Averaged power of 8–15-Hz oscillatory activity. Significant increases in 8–15-Hz oscillatory power were detected in all three structures. The pooled data from two monkeys were the same as those for the neuronal populations in Table 1. *** $P < 0.001$.

performed under the same general anesthesia as described above (Kaneda *et al.*, 2005). The MPTP injection (1.2 mg/kg) unilateral to the recording side was made through the common carotid artery with the external carotid artery clamped (Fig. 2A and B). With the monkey parkinsonian rating scale (Smith *et al.*, 1993; see also Supporting Information Data S1), motor signs were quantitatively evaluated (the maximum parkinsonian score was 20; that is, more serious parkinsonian stages were indicated by higher scores; Fig. 3A). To make moderate to severe parkinsonian models, monkeys received an additional carotid artery injection (1.0 mg/kg, 1 week after the first injection) and/or intravenous injections through the great saphenous vein (0.3 mg/kg every 4 days, 3 days after the last carotid injection). Monkey K received carotid injections twice (1.2 and 1.0 mg/kg) and intravenous injection once, and monkey Q received carotid injection once and intravenous injection four times. The total doses of MPTP were 2.5 mg/kg for monkey K and 2.4 mg/kg for monkey Q. Unit recordings of BG neurons in the parkinsonian state was started after the parkinsonian scores became stable, that is, 2 weeks (monkey K) and 3 weeks (monkey Q) after the final MPTP injection.

L-DOPA treatments

We investigated the effects of systemic dopamine administration on the neuronal activity of GPi/GPe and STN neurons in the parkinsonian state. After the control recordings of GPi/GPe and STN neurons, 3.5 mg/kg (monkey K) or 2.5 mg/kg (monkey Q) L-DOPA (DOP-ASTON, a dopamine precursor; Sankyo, Tokyo, Japan) was manually injected into the great saphenous vein at a low rate, and this was followed by the infusion of electrolyte fluid. To verify the contingency between the L-DOPA-induced behavioral effects and the activity changes in BG neurons, we avoided using Carbidopa, which could prevent the conversion of L-DOPA to dopamine peripherally and delay

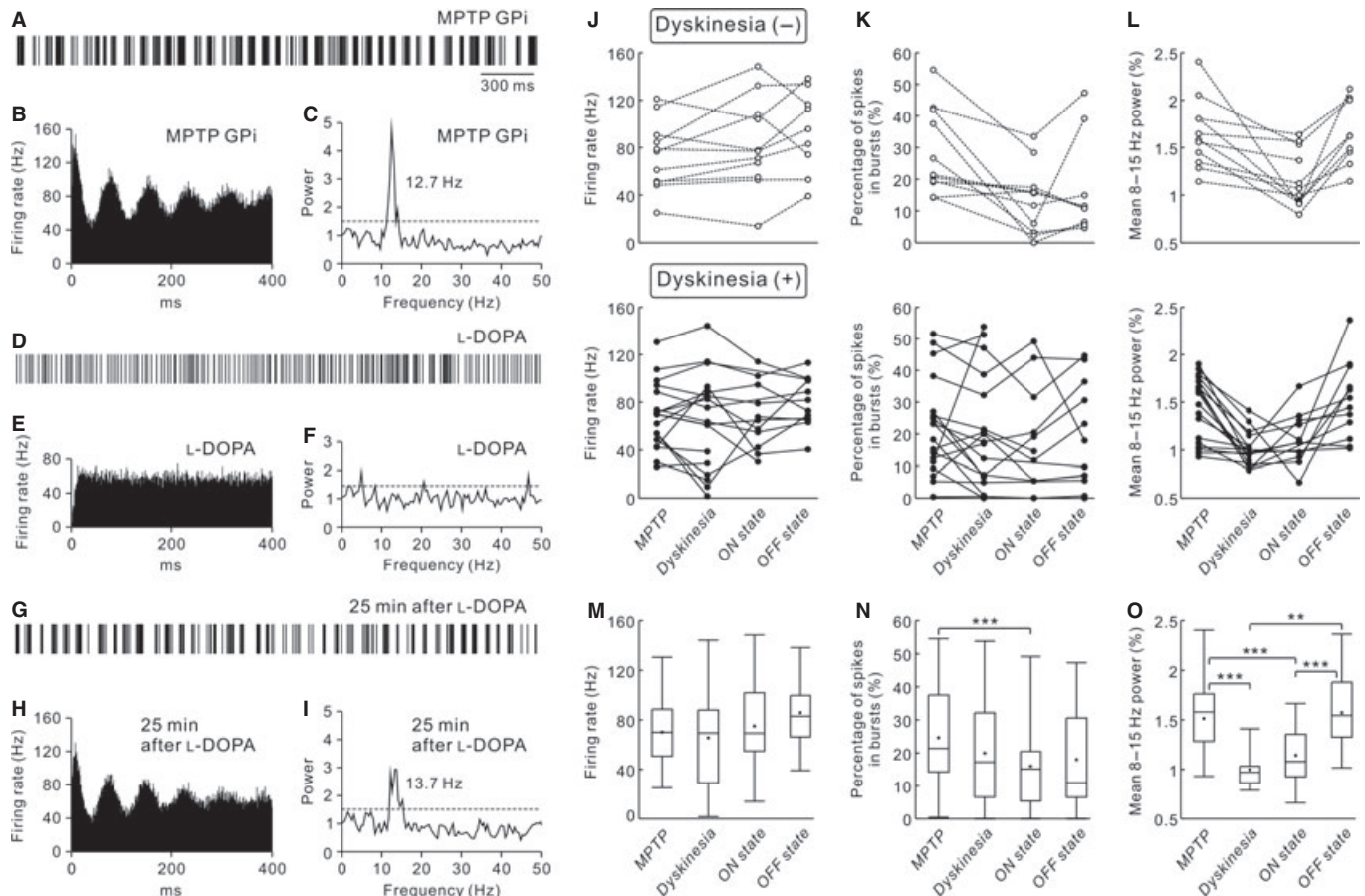


FIG. 5. L-DOPA effects on dopamine-depleted GPI neurons. (A, D and G) Representative 3-s digitized spikes from a 50-s spike train before and after intravenous L-DOPA injection. (B, E and H) Autocorrelograms calculated from the same spike train (bin width, 0.5 ms). (C, F and I) Power spectra of the same spike trains, compensated by the algorithm of Rivlin-Etzion *et al.* (2006b). Gray dashed lines represent a confidence level of $P = 0.01$. Peak frequency in the range of 8–15 Hz is also shown. A GPI neuron showed 8–15-Hz oscillations in the parkinsonian state (A–C). An intravenous L-DOPA injection reduced the 8–15-Hz oscillatory activity in the GPI (D–F), with an improvement in parkinsonian motor signs (ON state). Twenty-five minutes after the L-DOPA injection, the oscillatory activity resumed (G–I). At this time, recuperation from the parkinsonism was not observed (OFF state). (J–L) Changes in the spontaneous firing rate (J), the burst strength (K) and the mean 8–15-Hz power spectrum of spike trains (L) after the L-DOPA injections. The upper rows show the neurons recorded without dyskinesia. The lower rows show the neurons recorded with the development of dyskinesia. Data are plotted along the behavioral changes, and the data points from the same neuron are connected with lines. Owing to the excessive body movement of the monkeys, some GPI neurons were lost during neuronal recording. (M–O) Summaries of the L-DOPA effects on the firing rate (M), the burst strength (N) and the mean 8–15-Hz power (O) in 29 GPI neurons examined. In box plots, means are indicated as black dots. In this and subsequent figures, the repeated Wilcoxon signed-rank tests were performed to calculate statistically significant differences among pre-injection (labeled as MPTP) and post-injection (dyskinesia, ON state and OFF state) conditions. In the GPI neurons tested, the overall firing rate did not change throughout the injections. In contrast, the power of 8–15-Hz oscillations was significantly decreased from pre-injection states to dyskinetic states and to ON states. A significant decrease in the burst strength was also detected between pre-injection states and ON states. ** $P < 0.01$, *** $P < 0.001$.

the termination of the L-DOPA effects. An optimal dose of L-DOPA was determined so that the injection would reduce the gross parkinsonian scores by 5 or more. The L-DOPA effects on neuronal activity in the GPI/GPe and STN appeared within approximately 5 min. During this period, the L-DOPA greatly improved the motor symptoms of both monkeys, and eventually induced dyskinetic movements (dyskinetic state). The dyskinesia typically appeared as oral dyskinesia and/or forelimb dyskinesia, and sometimes spread to entire body parts. The excessive dyskinetic state usually ceased in 5–10 min and shifted to the ON state without dyskinesia, termed the 'ON state'. Approximately 30 min after the injection, the animals exhibited the original parkinsonism, termed the 'OFF state'. In some cases, the L-DOPA effects appeared without development of the dyskinetic state. The L-DOPA experiments were limited to two injections per recording day, and the interval between the injections was >2 h throughout the experiments. It should be noted that the electrophysiological data for the dopamine-depleted state in Table 1 were collected before the following receptor-

related drug injection experiments (monkey K, including the neurons sampled at least 48 h after the last L-DOPA injection; monkey Q, including the neurons recorded only in the L-DOPA-naïve state).

Unit recordings with local drug injection

We developed a microinjection method to examine the impacts of direct synaptic inputs (i.e. glutamatergic and GABAergic inputs) on the oscillatory activity of individual BG neurons. Unit recordings of GPI/GPe or STN neurons with local drug injection were performed with an electrode assembly consisting of a glass-coated Elgiloy microelectrode for unit recording and a silica tube for drug delivery, as described previously (Tachibana *et al.*, 2008). Through the silica tube, one of the following drugs was injected (0.03–0.05 $\mu\text{L}/\text{min}$; total, 0.1–0.2 μL): (i) a mixture of an *N*-methyl-D-aspartate receptor antagonist, 3-(2-carboxypiperazin-4-yl)-propyl-1-phosphonic acid (CPP) (1 mM; Sigma), and an AMPA/kainate

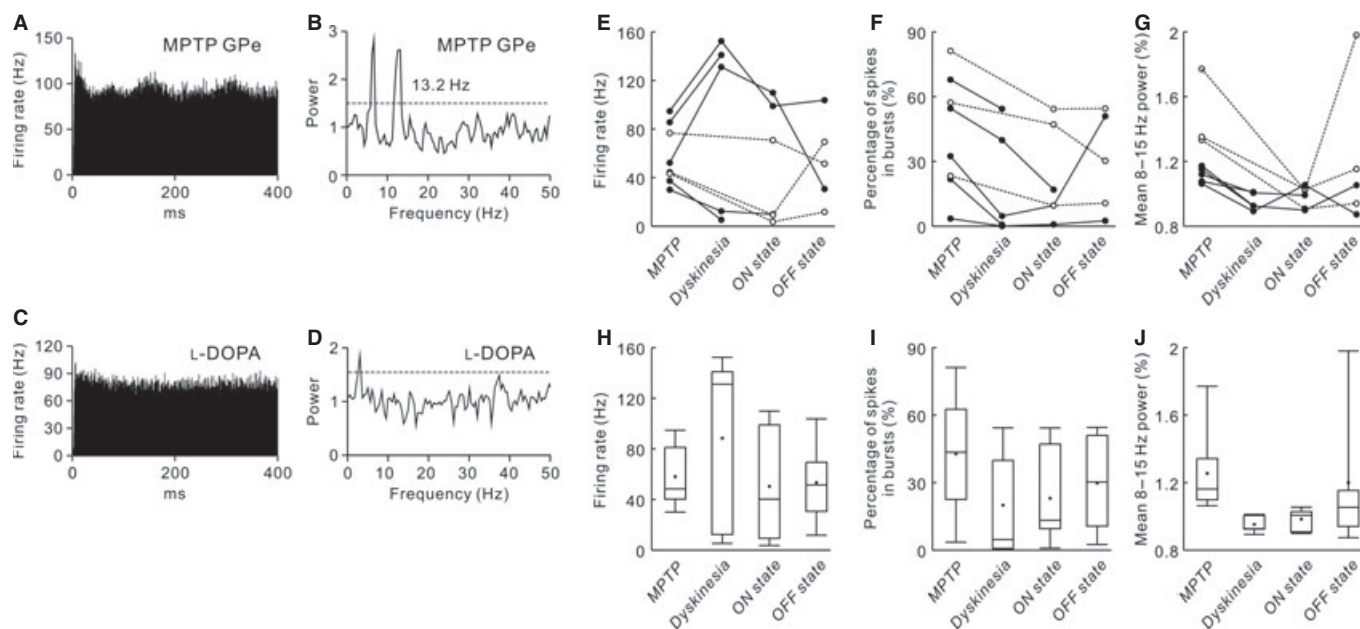


FIG. 6. L-DOPA effects on dopamine-depleted GPe neurons. (A and B) A GPe neuron showed 3–8-Hz and 8–15-Hz oscillations in the parkinsonian state. The conventions in this and the following figures are the same as in Fig. 5. (C and D) An intravenous L-DOPA injection suppressed both types of oscillation in the GPe neuron. (E–G) L-DOPA-induced changes in the spontaneous firing rate (E), the burst strength (F) and the mean 8–15-Hz power (G) of eight GPe neurons tested. Data from the neurons recorded without dyskinesia (open circles and broken lines) are superimposed on those from the neurons recorded with dyskinesia (filled circles and solid lines). (H–J) Summaries of the L-DOPA effects on the firing rate (H), the burst strength (I) and the mean 8–15-Hz power (J) in GPe neurons.

receptor antagonist, 1,2,3,4-tetrahydro-6-nitro-2,3-dioxo-benzo[*f*]quinoxaline-7-sulfonamide (NBQX) (1 mM; Sigma); and (ii) a GABA_A receptor antagonist, gabazine (1 mM; Sigma). Injection sites were located at least 1 mm apart because the effective radius of the drugs was estimated to be approximately 1 mm (Tachibana *et al.*, 2008). This method limited unit recordings to a maximum of two GPi/GPe neurons or a single STN neuron per recording day.

Methods for inactivation of the STN or GPe were similar to the methods described elsewhere (Nambu *et al.*, 2000; Tachibana *et al.*, 2008). A Teflon-coated tungsten wire that was attached to the 31-gauge needle of a 10- μ L Hamilton microsyringe, or the above electrode assembly, was inserted vertically into the STN or obliquely into the GPe with a hydraulic microdrive. A GABA_A receptor agonist, muscimol (4.4 mM; 0.5–1.0 μ L in the STN, 1–2 μ L in the GPe; Sigma), was injected. Because the effect of muscimol on the target structure lasted for several hours, the inactivation of the STN or GPe was limited to a single injection per recording day.

Data analysis

Off-line data analysis was performed with MATLAB software (MathWorks, Natick, MA, USA). Spontaneous firing rates and patterns of the recorded neurons were analyzed by calculating the autocorrelograms (bin width, 0.5 ms) from 50 s of digitized recordings.

Bursts of GPi/GPe and STN neurons were detected on the basis of the 'Poisson surprise' algorithm, with a 'surprise value' of at least three and a number of spikes of at least three in a burst (Wichmann & Soares, 2006; see also Supporting Information Fig. S1). Briefly, the algorithm can calculate a probability that successive spikes occur in a given time window of a spike train, which is assumed to be Poisson-distributed with the same firing rate. If the successive spikes occur with a significantly low probability ('surprise'), the spikes are considered as a burst. The strength of bursts was estimated by the

percentage of spikes in bursts (as compared with all spikes in the recording data), which has frequently been used in other studies (Levy *et al.*, 2001a; Wichmann & Soares, 2006). We also calculated the mean 'surprise value' of overall bursts detected by the algorithm. Oscillatory activity of GPi/GPe and STN neurons was estimated by spectral analysis of spike trains with a shuffling technique (Rivlin-Etzion *et al.*, 2006b). The method calculated the power spectral density (PSD) of spike trains based on Welch's method (Halliday *et al.*, 1995). The PSD calculation was performed with a non-overlapping Hann window with a length of 4096 bins. Because the sampling frequency of spike trains was 2 kHz, the frequency resolution was approximately 0.5 Hz. In the present study, the compensated PSD was obtained from the PSD of original spike trains divided by the mean PSD of locally ($T = 175$ – 225 ms) shuffled ($n = 50$) spike trains. The local shuffling method minimized the spectral distortion at lower frequencies caused by the refractory periods of neurons, and the effect of the neuronal firing rate on the PSD, thus enabling easy detection of periodic oscillatory phenomena in the recorded neurons. A confidence level ($P < 0.01$) of the compensated PSD was determined on the basis of the mean \pm standard deviation (SD) of the PSD values in the range of 270–300 Hz, at which the PSD values were stable. Oscillatory cells were defined by determining whether their two consecutive PSD values within individual ranges of 3–8 and 8–15 Hz crossed the confidence level (Soares *et al.*, 2004). The power (strength) of 3–8- and 8–15-Hz oscillations was estimated by averaging the PSD values within the individual frequency bands, and termed 'mean 3–8-Hz power' and 'mean 8–15-Hz power', respectively. We also estimated the oscillatory activity in the range of 20–30 Hz in the same manner.

Histology

At the end of the final recordings, reference lesions were placed at several sites by passing a cathodal DC current of 20 μ A through the

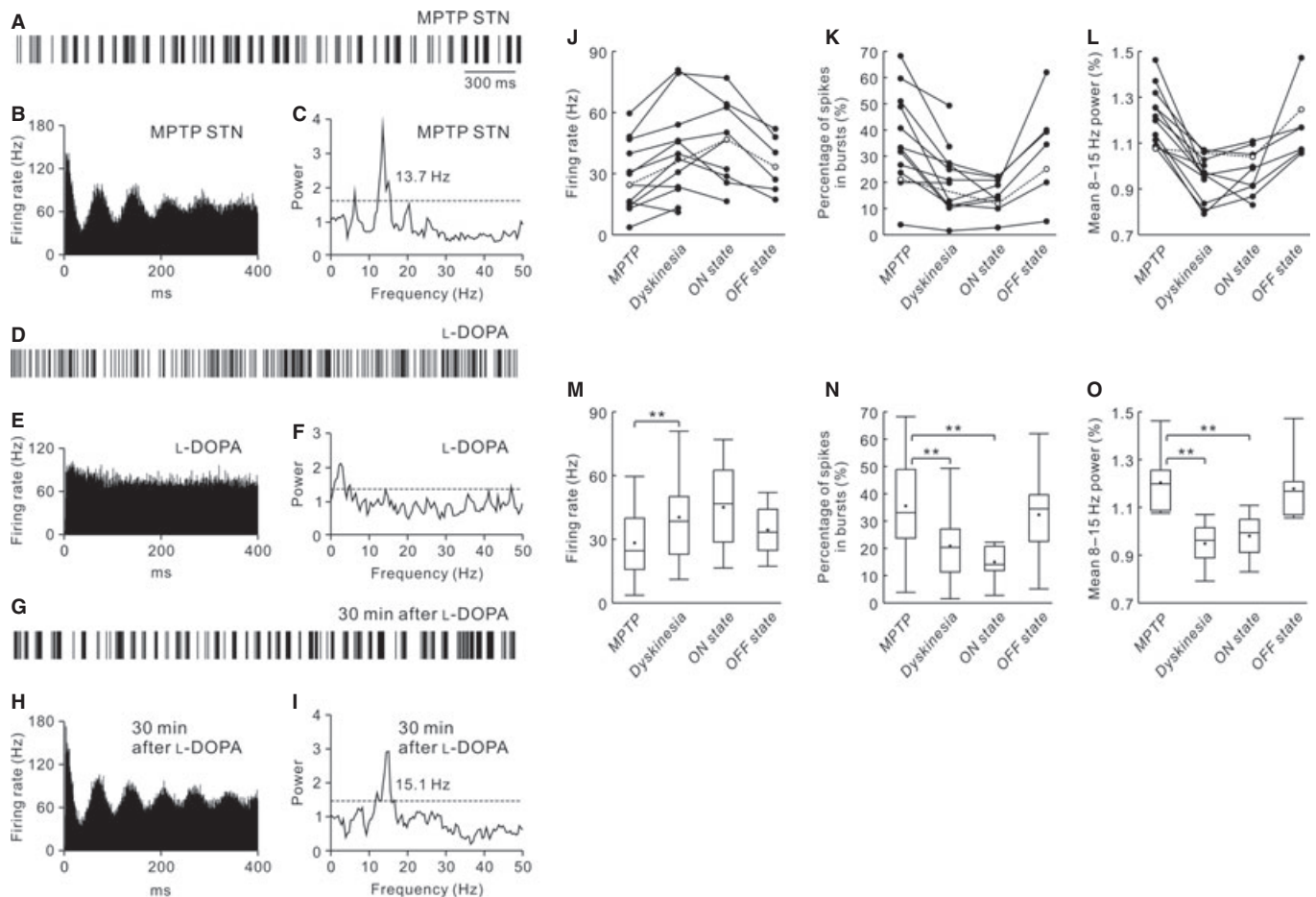


FIG. 7. L-DOPA effects on dopamine-depleted STN neurons. (A–C) An STN neuron showed oscillations in the parkinsonian state. (D–F) An intravenous L-DOPA injection increased the firing rate and suppressed the 8–15-Hz oscillatory activity of the STN neuron during the ON state. In this example, 3–8-Hz oscillations were also attenuated. (G–I) Thirty minutes after the L-DOPA injection, the oscillatory activity appeared again. (J–L) L-DOPA-induced changes in the spontaneous firing rate (J), the burst strength (K) and the mean 8–15-Hz power (L) of 13 STN neurons tested. Data from the neuron recorded without dyskinesia (open circles and broken lines) are superimposed on those from the neurons recorded with dyskinesia (filled circles and solid lines). (M–O) Summaries of the L-DOPA effects on the firing rate (M), the burst strength (N) and the mean 8–15-Hz power (O) in the STN neurons. The average firing rate was increased from pre-injection states to dyskinetic states. On the other hand, there were significant decreases in the burst strength and the mean power of 8–15-Hz oscillations from pre-injection states to dyskinetic states and to ON states. $^{**}P < 0.01$.

electrode for 30 s. The monkeys were deeply anesthetized with intravenous sodium pentobarbital (50 mg/kg) and perfused transcardially with the same methods as reported previously (Kaneda *et al.*, 2005). Serial 60- μ m sections were processed for Nissl staining or tyrosine hydroxylase (TH) immunostaining by the same methods as described elsewhere (Kaneda *et al.*, 2005; Tachibana *et al.*, 2008). The recording and drug injection sites were confirmed according to the lesions made by the cathodal DC current and the traces of electrode tracks.

Statistical analysis

All of the data are represented as mean \pm SD. Statistical tests were performed with SPSS (IBM, Armonk, NY, USA). Because we made an effort to minimize the damage to brain tissues caused by drug injections, the sample size was not large throughout the experiments. Therefore, we performed a non-parametric Wilcoxon signed-rank test or Mann–Whitney *U*-test for all neuronal data sets. The proportions of oscillatory cells in normal and parkinsonian states were compared by the use of Fisher's exact test. Significance levels were generally set as $P = 0.05$. In the studies with L-DOPA injections, however, we set the

significant levels at $P = 0.01$, because the Wilcoxon signed-rank tests were repeatedly performed.

Results

Behavioral and neuronal changes after MPTP injections

We produced the primate model of PD via a unilateral MPTP injection into the internal carotid artery and additional intravenous injections of MPTP. TH immunohistochemistry confirmed the loss of dopaminergic terminals in the putamen and dopaminergic neurons in the substantia nigra of the two MPTP-treated monkeys that served as subjects in this study (Fig. 2A and B). The reduction in TH immunoreactivity was more prominent in the ventral and lateral portions than in the dorsal and medial portions of the substantia nigra of MPTP-treated monkeys; selective loss of dopaminergic neurons by MPTP induction is commonly observed in human PD patients (Yamada *et al.*, 1990; Kaneda *et al.*, 2003). Both monkeys showed obvious parkinsonian signs, such as akinesia/bradykinesia, rigidity, and flexed posture, more severely on the side of the body contralateral to the carotid artery MPTP injection (Fig. 3A). Monkey

parkinsonian scores (Smith *et al.*, 1993; see also Supporting Information Data S1) of the contralateral side to the carotid injections were 11–12 in monkey K (contralateral side: tremor, 0–1/3; posture, 1/2; gait, 3/4; bradykinesia, 3/4; balance, 1/2; gross motor skill, 2/3; defense reaction, 1/2) (ipsilateral side: tremor, 0/3; bradykinesia, 3/4; gross motor skill, 2/3) and 13–14 in monkey Q (contralateral side: tremor, 0/3; posture, 2/2; gait, 3–4/4; bradykinesia, 3/4; balance, 1/2; gross motor skill, 3/3; defense reaction, 1/2) (ipsilateral side: tremor, 0/3; bradykinesia, 3/4; gross motor skill, 2/3). Monkey K occasionally showed weak limb tremor, with peak frequencies of 7.8 and 12.7 Hz (Fig. 3B) (see also Heimer *et al.*, 2006), whereas monkey Q showed no visible tremor. The parkinsonian scores were stable throughout the recording sessions.

Figure 4 and Table 1 show the electrophysiological properties of BG neurons in the normal and parkinsonian states. As compared with the normal state, the average firing rates of GPe and STN neurons in the parkinsonian state were significantly decreased and increased, respectively. However, no changes were detected in the firing rate of GPi neurons. Burst strength was increased from the normal to the parkinsonian state in the GPe, GPi, and STN. Both parkinsonian monkeys showed increases in the number of neurons that oscillated in the 8–15-Hz range in all three of the structures, whereas there were no consistent changes in the number of 3–8-Hz oscillatory cells. The mean power of the 8–15-Hz oscillations increased in all of the structures. Indeed, neurons in the GPi and STN of the two parkinsonian monkeys displayed remarkable tendencies to produce oscillatory bursts, as shown by rhythmic spike trains, and multiple peaks in the autocorrelograms, and power spectrum (e.g. Figs 5A–C and 7A–C). Although the power of 8–15-Hz oscillations in the GPe tended to be weaker than those in the GPi and STN, the oscillatory bursts were also observed in GPe neurons (Fig. 6). The peak frequency with a maximum power of the oscillatory bursts was approximately 13 Hz in all three structures in both monkeys. We also analyzed the power of 20–30-Hz oscillatory activity in the BG, but we did not find a significant increase from normal to parkinsonian conditions (monkey K, GPe, 0.87 ± 0.08 to 0.87 ± 0.15 ; monkey K, GPi, 0.86 ± 0.12 to 0.77 ± 0.14 ; monkey K, STN, 0.95 ± 0.06 to 0.84 ± 0.13 ; monkey Q, GPe, 0.83 ± 0.18 to 0.79 ± 0.15 ; monkey Q, GPi, 0.90 ± 0.12 to 0.81 ± 0.16 ; monkey Q, STN, 0.96 ± 0.08 to 0.84 ± 0.13 ; mean \pm SD). Thus, for the following drug injection studies, we pooled the neuronal data from two monkeys and focused on the 8–15-Hz oscillations.

Dopamine dependence of 8–15-Hz oscillations in the BG

We examined the effects of systemic dopamine administration on the neuronal activity of GPi/GPe and STN neurons under parkinsonian conditions (Fig. 1A). Across the L-DOPA injections tested, the behavioral effects appeared within 5 min, and parkinsonian motor scores (such as tremor, bradykinesia, and gross motor skill) were improved by 3–5 (ON state). In more than half of the cases, the animals developed dyskinetic movements in the orofacial and/or forelimb areas prior to the ON state (see Materials and methods). The excessive dyskinetic states usually ceased in 5–10 min. Approximately 30 min after each injection, the animals showed the original parkinsonism (OFF state). In a representative GPi neuron, an intravenous L-DOPA injection decreased the 8–15-Hz oscillations in the ON state (Fig. 5A–F), and the abnormal oscillations appeared again in the OFF state (Fig. 5G–I). In 29 GPi neurons examined, the overall firing rate was not changed throughout the injections (Fig. 5M; Wilcoxon signed-rank test). In contrast, the mean power

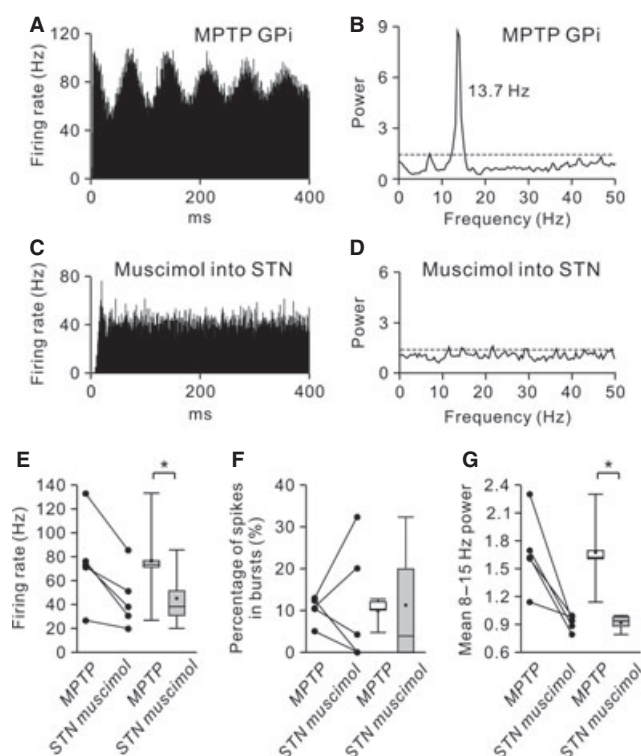


FIG. 8. Effects of STN inactivation on dopamine-depleted GPi neurons. (A and B) A GPi neuron showed abnormal oscillations in the parkinsonian state. (C and D) Muscimol inactivation of the STN decreased the firing rate, and suppressed 8–15-Hz oscillatory activity in the GPi. (E–G) Summaries of the effects of muscimol inactivation of the STN on the spontaneous firing rate (E), the burst strength (F) and the mean 8–15-Hz power spectrum of spike trains (G) in five GPi neurons examined. The STN inactivation significantly decreased the firing rate and the 8–15-Hz power of oscillations in the GPi. * $P < 0.05$.

of 8–15-Hz oscillations was significantly decreased from pre-injection states to dyskinetic states (Fig. 5O; $P < 0.001$, Wilcoxon signed-rank test) and to ON states ($P < 0.001$). Significant decreases in the burst strength were also detected between pre-injection states and ON states (Fig. 5N; $P < 0.001$, Wilcoxon signed-rank test). Although there was a tendency for the power of 8–15-Hz oscillations in dyskinetic states to be lower than that in ON states, we did not detect significant differences in the three parameters (i.e. firing rate, burst strength, and 8–15-Hz oscillatory power) between dyskinetic states and ON states. Similarly, the decreases in abnormal oscillatory bursts of GPe neurons were observed after L-DOPA injections, even though the average firing rate did not change across the recorded population (Fig. 6).

L-DOPA administration also suppressed 8–15-Hz oscillations in the STN (Fig. 7A–F). The abnormal oscillations were concomitant with the re-emergence of parkinsonian motor signs (Fig. 7G–I). In contrast to what was found for GPi/GPe neurons, the average firing rate of 13 STN neurons tested was increased from pre-injection states to dyskinetic states (Fig. 7M; $P = 0.005$). On the other hand, significant decreases in the burst strength (Fig. 7N) and the mean power of 8–15-Hz oscillations (Fig. 7O) were observed from pre-injection states to dyskinetic states ($P = 0.002$ for burst strength; $P = 0.002$ for 8–15-Hz oscillatory power) and to ON states ($P = 0.002$ for burst strength; $P = 0.008$ for 8–15-Hz oscillatory power). Thus far, we have demonstrated that abnormal burst firing and 8–15-Hz oscillatory activity in the GPi/GPe and STN are related to dopamine deficiency.

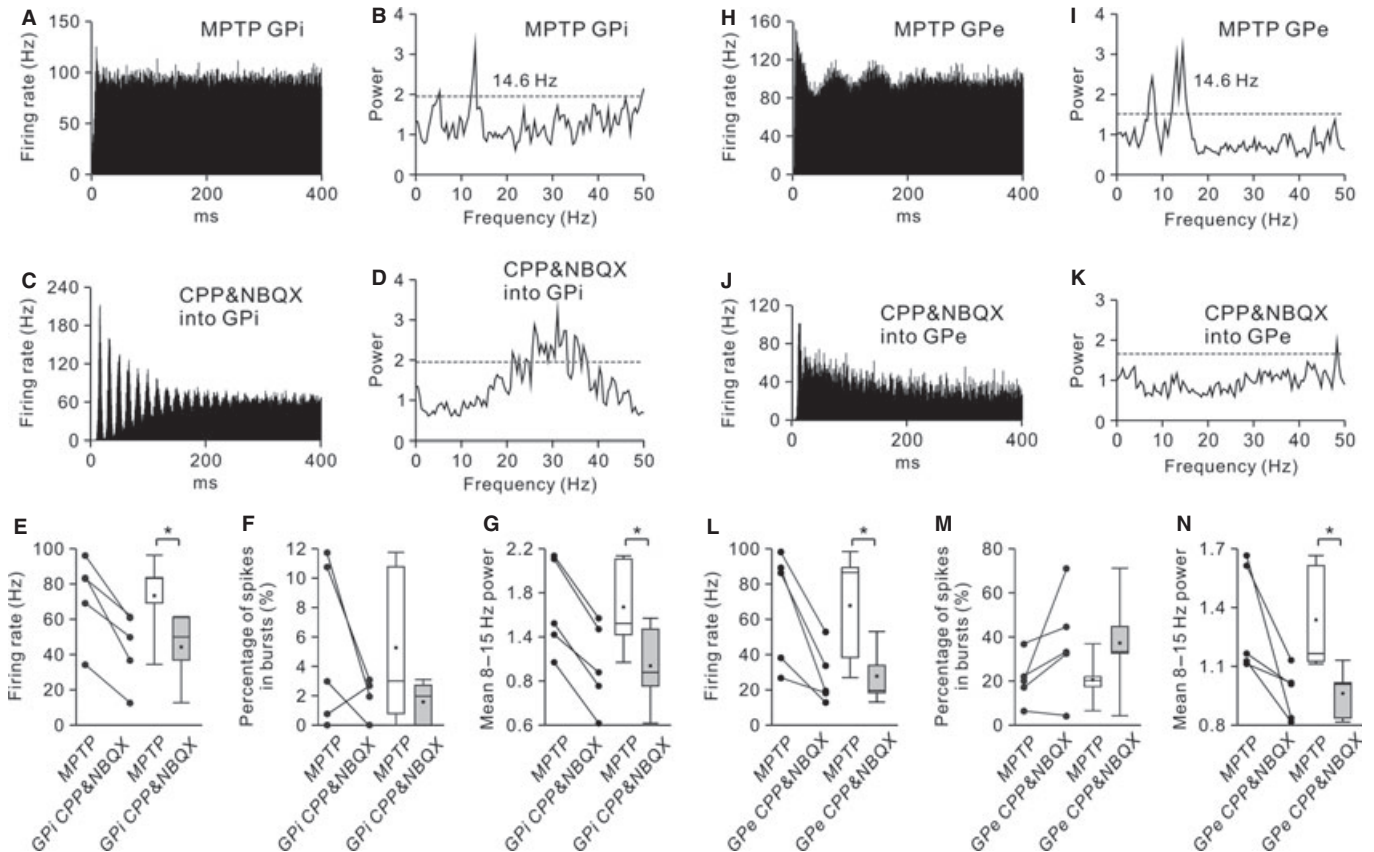


FIG. 9. Effects of intrapallidal blockade of ionotropic glutamatergic neurotransmission on dopamine-depleted GPI/GPe neurons. (A, B, H and I) A pallidal neuron (GPI, A and B; GPe, H and I) showed 3–8-Hz and 8–15-Hz oscillations in the parkinsonian state. (C, D, J and K) Microinjection of a mixture of CPP and NBQX in the vicinity of recorded GPI (C and D) and GPe (J and K) neurons decreased both the firing rates and oscillations. (E–G and L–N) Summaries of the effects of CPP and NBQX microinjections on the spontaneous firing rate (E and L), the burst strength (F and M) and the mean 8–15-Hz power spectrum of spike trains (G and N) in five GPI (E–G) and five GPe (L–N) neurons examined. Injections of CPP and NBQX significantly decreased the firing rate and the 8–15-Hz oscillatory power in the GPI and GPe. * $P < 0.05$.

Origins of abnormal 8–15-Hz oscillations in the GPI/GPe

The GPI and GPe receive glutamatergic inputs from the STN and GABAergic inputs from the striatum and/or GPe. To determine which inputs contribute to abnormal 8–15-Hz oscillations in the GPI, we first performed muscimol inactivation of the STN while simultaneously recording GPI neuronal activity (Fig. 1B). In all five cases, inactivation of the STN ameliorated parkinsonian motor signs, especially bradykinesia and rigidity, as previously reported (Bergman *et al.*, 1990; Wichmann *et al.*, 1994; Levy *et al.*, 2001b). The STN inactivation substantially decreased the 8–15-Hz oscillations (Fig. 8A–D and G; $P = 0.04$) and the firing rate (Fig. 8E; $P = 0.04$) in five GPI neurons, but no consistent changes were detected in the burst strength (Fig. 8F; $P = 0.89$). To obtain further evidence for subthalamic impacts on the oscillatory activity in the GPI/GPe, we also examined whether the intrapallidal blockade of ionotropic glutamate receptors could eliminate the GPI/GPe oscillations (Fig. 1C). Microinjection of a mixture of CPP and NBQX in the vicinity of recorded GPI/GPe neurons significantly decreased the average firing rate (Fig. 9A–D, H–K, E and L; $P = 0.04$ for both the GPI and GPe) and 8–15-Hz oscillations (Fig. 9G and N; $P = 0.04$ for both the GPI and GPe) in the GPI and GPe, whereas the burst strength was not changed uniformly in either structure (Fig. 9F and M; $P = 0.14$ for GPI; $P = 0.08$ for GPe).

We further tested whether GABAergic inputs from the striatum and/or GPe could affect the oscillatory activity of GPI/GPe neurons

(Fig. 1D). Microinjection of gabazine in the area surrounding recorded GPI/GPe neurons increased the firing rate of all of the neurons tested (Fig. 10A and C; $P = 0.02$ for GPI; $P = 0.04$ for GPe), and augmented the 8–15-Hz oscillations in the GPI (Fig. 10B; $P = 0.04$), but induced no significant changes in GPe oscillations (Fig. 10D; $P = 0.23$). The burst strength was not changed after the injections (GPI, $n = 7$, $P = 0.17$, Wilcoxon signed-rank test; GPe, $n = 5$, $P = 0.14$, Wilcoxon signed-rank test; data not shown). These results suggest that 8–15-Hz oscillations in the GPI/GPe originate from glutamatergic inputs mainly from the STN.

Origins of abnormal 8–15-Hz oscillations in the STN

The STN is known to receive glutamatergic inputs from the cerebral cortex and the thalamus, and GABAergic inputs from the GPe (Kitai & Deniau, 1981; Kita *et al.*, 1983; Bevan *et al.*, 1995). We first tested whether the elimination of ionotropic glutamatergic inputs could affect the generation of abnormal oscillatory activity in the STN (Fig. 1E). Local injections of a mixture of CPP and NBQX in the vicinity of recorded neurons suppressed the 8–15-Hz oscillations (Fig. 11A–D and G; $P = 0.03$), but increased their burst activities (Fig. 11F; $P = 0.03$), in six STN neurons tested. Such local injections did not induce consistent changes in the firing rate (Fig. 11E; $P = 0.84$).

We further examined whether the interruption of GPe-derived GABAergic inputs can suppress oscillations in the STN (Fig. 1F).

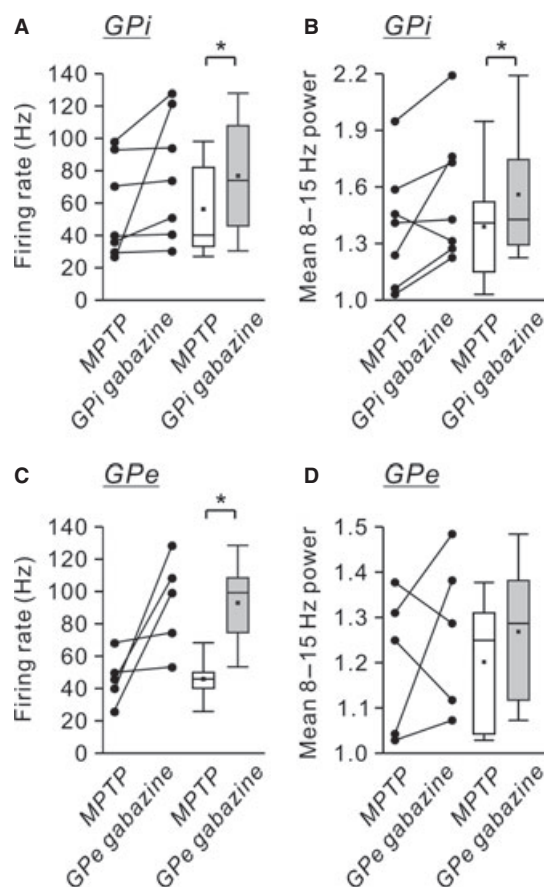


FIG. 10. Effects of intrapallidal blockade of ionotropic GABAergic neurotransmission on dopamine-depleted GPi/GPe neurons. Effects of intrapallidal gabazine microinjections on the spontaneous firing rate (A and C) and the mean 8–15-Hz power spectrum of spike trains (B and D) in seven GPi (A and B) and five GPe (C and D) neurons examined in the parkinsonian state. Injections of gabazine significantly increased the firing rates of GPi/GPe neurons, and increased the 8–15-Hz oscillatory power in the GPi. $*P < 0.05$.

Muscimol inactivation of the GPe attenuated the 8–15-Hz oscillations (Fig. 12A–D and G; $P = 0.03$) and the burst strength (Fig. 12F; $P = 0.03$), and increased the firing rate (Fig. 12E; $P = 0.03$), in six STN neurons tested. In contrast to muscimol inactivation of the STN, the GPe inactivation induced no clear behavioral changes. Taking these findings together, we conclude that the STN oscillatory rhythm is generated by both glutamatergic and GABAergic inputs to the STN.

Discussion

Our results show that loss of nigral dopamine neurons induced abnormal oscillations of GPi/GPe and STN neurons. The GPi/GPe and STN oscillations were reversed by systemic dopamine administration. Notably, direct manipulations of synaptic transmission within the BG of awake parkinsonian primates showed that STN oscillations induced oscillatory activity in the 8–15-Hz range in the GPi/GPe. We further demonstrated that the STN oscillations were strongly driven by (i) glutamatergic inputs, which are thought to arise mainly from the cortex, and (ii) GABAergic inputs from the GPe. These findings suggest that, in the dopamine-depleted state, glutamatergic inputs to the STN and reciprocal GPe–STN interconnections are both important for the generation and amplification of the oscillatory activity of STN neurons, which is subsequently transmitted to the GPi (Fig. 13).

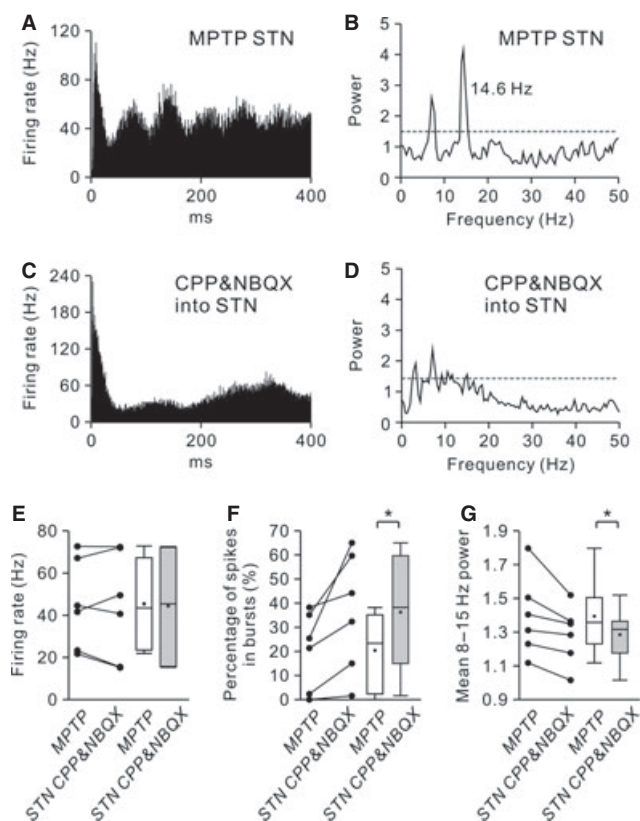


FIG. 11. Effects of intrasubthalamic blockade of ionotropic glutamatergic neurotransmission on dopamine-depleted STN neurons. (A and B) An STN neuron showed abnormal oscillatory bursts in the parkinsonian state. (C and D) Intrasubthalamic microinjection of a mixture of CPP and NBQX decreased 3–8-Hz and 8–15-Hz oscillations in the STN. On the other hand, the injection increased burst firing of the neuron. (E–G) Summaries of the effects of intrasubthalamic microinjections of CPP and NBQX on the spontaneous firing rate (E), the burst strength (F) and the mean 8–15-Hz power spectrum of spike trains (G) in six STN neurons examined. The microinjections of CPP and NBQX significantly decreased the 8–15-Hz oscillatory power, but increased the burst strength in the STN. $*P < 0.05$.

The classic model of PD pathophysiology suggests that degeneration of dopaminergic neurons leads to suppression of the striato-GPi ‘direct’ pathway and enhancement of the striato-GPe ‘indirect’ pathway; the increased GPi outputs attenuate thalamocortical neuron activity and induce parkinsonian motor signs (Albin *et al.*, 1989; DeLong, 1990). In this study, two MPTP-treated monkeys exhibited significant firing rate changes in STN neurons, but not in GPi neurons. Several reviews have emphasized that parkinsonism is directly related to BG oscillations (Boraud *et al.*, 2002; Brown, 2003; Gatev *et al.*, 2006; Rivlin-Etzion *et al.*, 2006a; Hammond *et al.*, 2007). The first goal of the present study was to test whether the abnormal BG oscillations depend on dopaminergic inputs. We confirmed that abnormal 8–15-Hz oscillations were increased in the GPi/GPe and STN of dopamine-depleted monkey brain, and were reversed after intravenous L-DOPA injections, with improvements in parkinsonian signs (Heimer *et al.*, 2006). Contrary to expectations, the firing rate of STN neurons increased following the L-DOPA injections. As in the striatum, L-DOPA might be converted to dopamine, which could be released from axon terminals of the remaining dopaminergic and serotonergic neurons in the STN (Lavoie & Parent, 1990; Francois *et al.*, 2000; Bezard *et al.*, 2001). Thus, L-DOPA could increase the firing rate of monkey

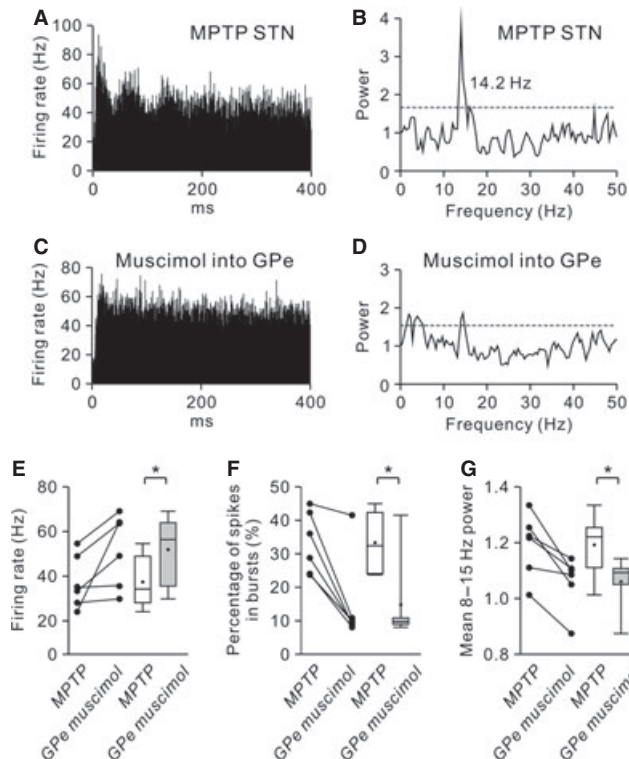


FIG. 12. Effects of GPe inactivation on dopamine-depleted STN neurons. (A and B) An STN neuron showed abnormal 8–15-Hz oscillations in the parkinsonian state. (C and D) Muscimol inactivation of the GPe decreased the 8–15-Hz oscillations in the STN, with an increase in the firing rate. (E–G) Summaries of the effects of muscimol inactivation of the GPe on the spontaneous firing rate (E), the burst strength (F) and the mean 8–15-Hz power spectrum of spike trains (G) in six STN neurons examined. Across the recorded population, the burst strength and the 8–15-Hz oscillations in the STN were decreased after GPe inactivation, whereas the GPe inactivation increased the firing rates of STN neurons. * $P < 0.05$.

STN neurons by eliciting the presynaptic suppression of GABAergic inputs via the direct activation of D2-like receptors (Shen & Johnson, 2000, 2005; Baufreton & Bevan, 2008).

We may predict that L-DOPA injections could reverse the decrease in the GPe firing rate after MPTP treatment. In contrast to previous reports that L-DOPA injections reversed the decrease in the rate of GPe neuron firing after MPTP treatment (Boraud *et al.*, 1998; Heimer *et al.*, 2006), we could not detect such a change uniformly. Increased STN activity may excite some GPe neurons, which may then inhibit other neighboring GPe neurons through GPe–GPe intranuclear axon collaterals (Kita & Kitai, 1994; Nambu & Llinás, 1997; Sato *et al.*, 2000). The data obtained from our L-DOPA studies suggest that normalization of neuronal oscillations in the GPi/GPe and STN may be more critical for L-DOPA actions in parkinsonian signs than changes in their spontaneous firing rates.

Our next aim was to determine the origin of 8–15-Hz oscillations of GPi/GPe neurons. The GPi/GPe receives glutamatergic inputs mainly from the STN and striatal GABAergic inputs (for review, see Smith *et al.*, 1998). The GPi/GPe also receives GABAergic inputs from the GPe through the GPe–GPi projection and the intranuclear collaterals (Hazrati *et al.*, 1990). However, no studies have demonstrated coherent activity between striatal projection neurons and GPi/GPe neurons. Here, we hypothesized that the GPi/GPe oscillations may be generated by glutamatergic inputs from the STN. Our findings revealed that STN inactivation simultaneously decreased the firing rate

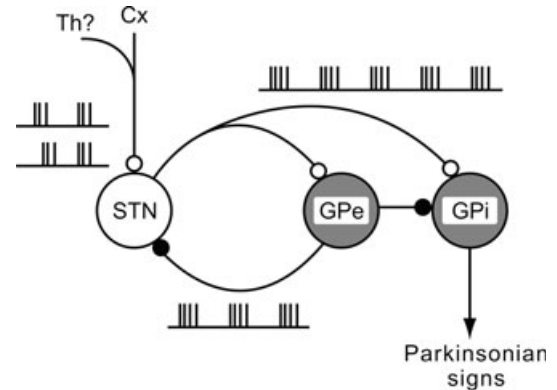


FIG. 13. Schematic diagram showing neural circuits involved in the generation of BG oscillations. In the dopamine-depleted state, a cooperative action of glutamatergic inputs from the cortex (Cx) [and perhaps also from the thalamus (Th)] and reciprocal GPe–STN interconnections can generate and amplify the oscillatory activity of STN neurons. The STN oscillations are finally transmitted to the GPi, thus contributing to the expression of parkinsonian motor signs. Open and filled circles represent glutamatergic and GABAergic synapses, respectively.

of GPi neurons, dampened their 8–15-Hz oscillations, and improved parkinsonian motor signs (see also Wichmann *et al.*, 1994). Moreover, microinjection of ionotropic glutamate receptor antagonists reduced the spontaneous firing rate and oscillatory activity in GPi/GPe neurons. In contrast, the 8–15-Hz oscillations were exaggerated or unchanged after microinjection of an ionotropic GABA receptor antagonist. These data suggest that the oscillatory events of GPi/GPe neurons are generated by glutamatergic inputs mainly from the STN, but not by GABAergic inputs from the striatum and GPe.

The final objective of this study was to elucidate the origin of 8–15-Hz oscillations in the STN. The glutamatergic afferents of the STN, which originate from the cortex and the thalamus, constitute one possibility (Kitai & Deniau, 1981; Bevan *et al.*, 1995). The present data showed that the STN oscillations were suppressed after the intrasubthalamic microinjection of ionotropic glutamate receptor antagonists. This suggests that the STN oscillations are partly formed by glutamatergic inputs to the STN. In accordance with the present result, estimates of coherence between the electrocorticogram and the STN LFPs/STN unit activity in the parkinsonian state have suggested that cortical glutamatergic inputs can drive STN oscillations in frequency bands below 30 Hz (Magill *et al.*, 2000, 2001; Sharott *et al.*, 2005; Mallet *et al.*, 2008b). The other possible glutamatergic sources of the primate STN are the intralaminar thalamic nuclei (Lanciego *et al.*, 2009). The parafascicular thalamic nucleus (PF) neurons in the rat PD model show some increased oscillatory activity (in the 0.5–2.5-Hz range) as compared with controls, but simultaneous recording of STN and PF neurons indicates that a majority of PF neurons fire after STN firing (Parr-Brownlie *et al.*, 2009). The contribution of thalamostriatal glutamatergic afferents to STN oscillations needs to be further elucidated. Another candidate for the origin of STN oscillations comprises the GABAergic inputs from the GPe, which is interconnected with the STN (Baufreton *et al.*, 2005a). A recent *in vivo* rat study has indicated that dopamine depletion develops the 15–30-Hz oscillations between single GPe–STN neuron pairs (Mallet *et al.*, 2008a). We demonstrated that muscimol inactivation of the GPe attenuated the 8–15-Hz oscillatory activity of STN neurons and suppressed their burst firing properties. This result indicates that the GABAergic inputs from the GPe are likely to contribute to the production of the 8–15-Hz oscillatory bursts in the STN. The decrease in dopaminergic innervation of the GPe in MPTP-

treated monkeys (Schneider & Dacko, 1991) can augment the GPe–GPe GABAergic transmission (Watanabe *et al.*, 2009). The glutamatergic inputs with synchronized GABAergic inputs from the GPe may accelerate the rhythmic phase-locked activity in parkinsonian STN neurons, where dopaminergic innervation of the STN is lacking (Shen & Johnson, 2000, 2005; Baufreton *et al.*, 2005b; Baufreton & Bevan, 2008).

The present study focused on the 8–15-Hz oscillations in the BG of parkinsonian monkeys. LFPs recorded from the GPi/GPe and STN of parkinsonian rodents and PD patients exhibit dopamine-dependent synchronization in the higher 15–30-Hz range (Brown *et al.*, 2001; Cassidy *et al.*, 2002; Sharott *et al.*, 2005; Mallet *et al.*, 2008a,b). Single-unit recordings in the STN of PD patients, however, have demonstrated neuronal oscillations in the frequency range of 10–25 Hz (Levy *et al.*, 2000, 2002), similar to those in MPTP-treated monkeys. The discrepancy in peak frequencies among oscillation/synchronization might be attributable to the difference in the recording setup (Levy *et al.*, 2002), the extent to which loss of dopamine (including other catecholamines) progresses, depending on how parkinsonism is induced (Meredith *et al.*, 2008), and the species-specific intrinsic membrane properties of individual BG neurons and/or emergent properties of the cortico-BG circuit. The BG oscillations in the range below 30 Hz may constrain cortical processing via the BG-thalamocortical pathways (Engel & Fries, 2010). On the other hand, Leblois *et al.* (2007) have reported that oscillatory activity of BG neurons appears after the emergence of severe parkinsonian signs, and concluded that a causal relationship between BG oscillations and PD symptoms is unlikely. There is a possibility that the BG oscillations may merely reflect sensory inputs from the periphery in the states of akinesia/bradykinesia, rigidity, and tremor (Baker, 2007). Here, we simply emphasize that the BG oscillations disappeared when parkinsonian signs were alleviated. In fact, therapeutic approaches, such as dopaminergic medication and STN stimulation, and self-generated movements in human patients are known to decrease the cortico-BG synchronization (Brown *et al.*, 2001, 2004; Cassidy *et al.*, 2002; Levy *et al.*, 2002; Williams *et al.*, 2002; Silberstein *et al.*, 2005; Lafreniere-Roula *et al.*, 2010). In a similar manner, the suppression of the 8–15-Hz oscillations in the primate BG might be required to improve parkinsonian motor signs. We should also mention that BG dysfunction is associated with the abnormal ‘dynamic’ network properties in the dopamine-depleted BG, owing to the imbalance of neuronal processing between the ‘enhanced’ cortico-STN-GPi hyperdirect pathway and the ‘attenuated’ cortico-striato-GPi direct pathway. The BG oscillations generated in the hyperdirect pathway are suggested to serve to limit the ‘action selection’ properties processed in the direct pathway (Leblois *et al.*, 2006). In addition to the present data showing that STN inactivation suppressed the BG oscillations, our recent studies have revealed that cortically evoked inhibition in the GPi, which is induced via the direct pathway and associated with motor execution (Nambu *et al.*, 2000), is attenuated in the parkinsonian state and restored after STN inactivation (Nambu *et al.*, 2005; Kita & Kita, 2011). These findings suggest the importance of suppression of the ‘enhanced’ hyperdirect pathway in the reversal of parkinsonian motor signs. Our findings may shed light on the pathophysiology of PD and the exact mechanisms of many current therapies, and will help to develop improved treatments for PD patients.

Supporting Information

Additional supporting information may be found in the online version of this article:

Fig. S1. Three examples of burst detection using the ‘Poisson surprise’ algorithm.

Data S1. Behavioral criteria of the primate parkinsonian rating scale.

Please note: As a service to our authors and readers, this journal provides supporting information supplied by the authors. Such materials are peer-reviewed and may be re-organized for online delivery, but are not copy-edited or typeset by Wiley-Blackwell. Technical support issues arising from supporting information (other than missing files) should be addressed to the authors.

Acknowledgements

This study was supported by Grants-in-Aid for Scientific Research from the Ministry of Education, Culture, Sports, Science and Technology of Japan, the Japan Intractable Diseases Research Foundation and Hori Information Science Promotion Foundation to Y. Tachibana and A. Nambu, and NIH grants (NS-47085 and NS-57236) to H. Kita. We thank S. Yamamoto and I. Monosov for helpful comments and discussion, M. Meitzler for editing the manuscript, A. Ito, K. Miyamoto and M. Imanishi for technical assistance, and H. Toyoda for MRI scans.

Abbreviations

BG, basal ganglia; CPP, 3-(2-carboxypiperazin-4-yl)-propyl-1-phosphonic acid; GPe, external segment of the globus pallidus; GPi, internal segment of the globus pallidus; L-DOPA, L-3,4-dihydroxyphenylalanine; LFP, local field potential; MPTP, 1-methyl-4-phenyl-1,2,3,6-tetrahydropyridine; NBQX, 1,2,3,4-tetrahydro-6-nitro-2,3-dioxo-benzof[quinoxaline-7-sulfonamide; PD, Parkinson's disease; PF, parafascicular thalamic nucleus; PSD, power spectral density; SD, standard deviation; STN, subthalamic nucleus; TH, tyrosine hydroxylase.

References

- Albin, R.L., Young, A.B. & Penney, J.B. (1989) The functional anatomy of basal ganglia disorders. *Trends Neurosci.*, **12**, 366–375.
- Baker, S.N. (2007) Oscillatory interactions between sensorimotor cortex and the periphery. *Curr. Opin. Neurobiol.*, **17**, 649–655.
- Baufreton, J. & Bevan, M.D. (2008) D2-like dopamine receptor-mediated modulation of activity-dependent plasticity at GABAergic synapses in the subthalamic nucleus. *J. Physiol.*, **586**, 2121–2142.
- Baufreton, J., Atherton, J.F., Surmeier, D.J. & Bevan, M.D. (2005a) Enhancement of excitatory synaptic integration by GABAergic inhibition in the subthalamic nucleus. *J. Neurosci.*, **25**, 8505–8517.
- Baufreton, J., Zhu, Z.T., Garret, M., Bioulac, B., Johnson, S.W. & Taupignon, A.I. (2005b) Dopamine receptors set the pattern of activity generated in subthalamic neurons. *FASEB J.*, **19**, 1771–1777.
- Bergman, H., Wichmann, T. & DeLong, M.R. (1990) Reversal of experimental parkinsonism by lesions of the subthalamic nucleus. *Science*, **249**, 1436–1438.
- Bergman, H., Wichmann, T., Karmon, B. & DeLong, M.R. (1994) The primate subthalamic nucleus. II. Neuronal activity in the MPTP model of parkinsonism. *J. Neurophysiol.*, **72**, 507–520.
- Bevan, M.D., Francis, C.M. & Bolam, J.P. (1995) The glutamate-enriched cortical and thalamic input to neurons in the subthalamic nucleus of the rat: convergence with GABA-positive terminals. *J. Comp. Neurol.*, **361**, 491–511.
- Bezard, E., Brotchie, J.M. & Gross, C.E. (2001) Pathophysiology of levodopa-induced dyskinesia: potential for new therapies. *Nat. Rev. Neurosci.*, **2**, 577–588.
- Boraud, T., Bezard, E., Guehl, D., Bioulac, B. & Gross, C. (1998) Effects of L-DOPA on neuronal activity of the globus pallidus externus (GPe) and globus pallidus internus (GPi) in the MPTP-treated monkey. *Brain Res.*, **787**, 157–160.
- Boraud, T., Bezard, E., Bioulac, B. & Gross, C.E. (2002) From single extracellular unit recording in experimental and human Parkinsonism to the development of a functional concept of the role played by the basal ganglia in motor control. *Prog. Neurobiol.*, **66**, 265–283.
- Brown, P. (2003) Oscillatory nature of human basal ganglia activity: relationship to the pathophysiology of Parkinson's disease. *Mov. Disord.*, **18**, 357–363.

- Brown, P., Oliviero, A., Mazzone, P., Insola, A., Tonali, P. & Di Lazzaro, V. (2001) Dopamine dependency of oscillations between subthalamic nucleus and pallidum in Parkinson's disease. *J. Neurosci.*, **21**, 1033–1038.
- Brown, P., Mazzone, P., Oliviero, A., Altibrandi, M.G., Pilato, F., Tonali, P.A. & Di Lazzaro, V. (2004) Effects of stimulation of the subthalamic area on oscillatory pallidal activity in Parkinson's disease. *Exp. Neurol.*, **188**, 480–490.
- Cassidy, M., Mazzone, P., Oliviero, A., Insola, A., Tonali, P., Di Lazzaro, V. & Brown, P. (2002) Movement-related changes in synchronization in the human basal ganglia. *Brain*, **125**, 1235–1246.
- DeLong, M.R. (1990) Primate models of movement disorders of basal ganglia origin. *Trends Neurosci.*, **13**, 281–285.
- Engel, A.K. & Fries, P. (2010) Beta-band oscillations – signalling the status quo? *Curr. Opin. Neurobiol.*, **20**, 156–165.
- Filion, M. (1979) Effects of interruption of the nigrostriatal pathway and of dopaminergic agents on the spontaneous activity of globus pallidus neurons in the awake monkey. *Brain Res.*, **178**, 425–441.
- Francois, C., Savy, C., Jan, C., Tande, D., Hirsch, E.C. & Yelnik, J. (2000) Dopaminergic innervation of the subthalamic nucleus in the normal state, in MPTP-treated monkeys, and in Parkinson's disease patients. *J. Comp. Neurol.*, **425**, 121–129.
- Gatev, P., Darbin, O. & Wichmann, T. (2006) Oscillations in the basal ganglia under normal conditions and in movement disorders. *Mov. Disord.*, **21**, 1566–1577.
- Halliday, D.M., Rosenberg, J.R., Amjad, A.M., Breeze, P., Conway, B.A. & Farmer, S.F. (1995) A framework for the analysis of mixed time series/point process data-theory and application to the study of physiological tremor, single motor unit discharges and electromyograms. *Prog. Biophys. Mol. Biol.*, **64**, 237–278.
- Hammond, C., Bergman, H. & Brown, P. (2007) Pathological synchronization in Parkinson's disease: networks, models and treatments. *Trends Neurosci.*, **30**, 357–364.
- Hazrati, L.N., Parent, A., Mitchell, S. & Haber, S.N. (1990) Evidence for interconnections between the two segments of the globus pallidus in primates: a PHA-L anterograde tracing study. *Brain Res.*, **533**, 171–175.
- Heimer, G., Rivlin-Etzion, M., Bar-Gad, I., Goldberg, J.A., Haber, S.N. & Bergman, H. (2006) Dopamine replacement therapy does not restore the full spectrum of normal pallidal activity in the 1-methyl-4-phenyl-1,2,3,6-tetra-hydropyridine primate model of Parkinsonism. *J. Neurosci.*, **26**, 8101–8114.
- Kaneda, K., Imanishi, M., Nambu, A., Shigemoto, R. & Takada, M. (2003) Differential expression patterns of mGluR1 α in monkey nigral dopamine neurons. *Neuroreport*, **14**, 947–950.
- Kaneda, K., Tachibana, Y., Imanishi, M., Kita, H., Shigemoto, R., Nambu, A. & Takada, M. (2005) Down-regulation of metabotropic glutamate receptor 1 α in globus pallidus and substantia nigra of parkinsonian monkeys. *Eur. J. Neurosci.*, **22**, 3241–3254.
- Kita, H. & Kita, T. (2011) Cortical stimulation evokes abnormal responses in the dopamine-depleted rat basal ganglia. *J. Neurosci.*, **31**, 10311–10322.
- Kita, H. & Kitai, S.T. (1994) The morphology of globus pallidus projection neurons in the rat: an intracellular staining study. *Brain Res.*, **636**, 308–319.
- Kita, H., Chang, H.T. & Kitai, S.T. (1983) Pallidal inputs to subthalamus: intracellular analysis. *Brain Res.*, **264**, 255–265.
- Kitai, S.T. & Deniau, J.M. (1981) Cortical inputs to the subthalamus: intracellular analysis. *Brain Res.*, **214**, 411–415.
- Lafreniere-Roula, M., Darbin, O., Hutchison, W.D., Wichmann, T., Lozano, A.M. & Dostrovsky, J.O. (2010) Apomorphine reduces subthalamic neuronal entropy in parkinsonian patients. *Exp. Neurol.*, **225**, 455–458.
- Lanciego, J.L., Lopez, I.P., Rico, A.J., Aymerich, M.S., Perez-Manso, M., Conte, L., Combarro, C., Roda, E., Molina, C., Gonzalo, N., Castle, M., Tunon, T., Erro, E. & Barroso-Chinea, P. (2009) The search for a role of the caudal intralaminar nuclei in the pathophysiology of Parkinson's disease. *Brain Res. Bull.*, **78**, 55–59.
- Lavoie, B. & Parent, A. (1990) Immunohistochemical study of the serotonergic innervation of the basal ganglia in the squirrel monkey. *J. Comp. Neurol.*, **299**, 1–16.
- Leblois, A., Boraud, T., Meissner, W., Bergman, H. & Hansel, D. (2006) Competition between feedback loops underlies normal and pathological dynamics in the basal ganglia. *J. Neurosci.*, **26**, 3567–3583.
- Leblois, A., Meissner, W., Bioulac, B., Gross, C.E., Hansel, D. & Boraud, T. (2007) Late emergence of synchronized oscillatory activity in the pallidum during progressive Parkinsonism. *Eur. J. Neurosci.*, **26**, 1701–1713.
- Levy, R., Hutchison, W.D., Lozano, A.M. & Dostrovsky, J.O. (2000) High-frequency synchronization of neuronal activity in the subthalamic nucleus of parkinsonian patients with limb tremor. *J. Neurosci.*, **20**, 7766–7775.
- Levy, R., Dostrovsky, J.O., Lang, A.E., Sime, E., Hutchison, W.D. & Lozano, A.M. (2001a) Effects of apomorphine on subthalamic nucleus and globus pallidus internus neurons in patients with Parkinson's disease. *J. Neurophysiol.*, **86**, 249–260.
- Levy, R., Lang, A.E., Dostrovsky, J.O., Pahapill, P., Romas, J., Saint-Cyr, J., Hutchison, W.D. & Lozano, A.M. (2001b) Lidocaine and muscimol microinjections in subthalamic nucleus reverse Parkinsonian symptoms. *Brain*, **124**, 2105–2118.
- Levy, R., Ashby, P., Hutchison, W.D., Lang, A.E., Lozano, A.M. & Dostrovsky, J.O. (2002) Dependence of subthalamic nucleus oscillations on movement and dopamine in Parkinson's disease. *Brain*, **125**, 1196–1209.
- Magill, P.J., Bolam, J.P. & Bevan, M.D. (2000) Relationship of activity in the subthalamic nucleus–globus pallidus network to cortical electroencephalogram. *J. Neurosci.*, **20**, 820–833.
- Magill, P.J., Bolam, J.P. & Bevan, M.D. (2001) Dopamine regulates the impact of the cerebral cortex on the subthalamic nucleus–globus pallidus network. *Neuroscience*, **106**, 313–330.
- Mallet, N., Pogossyan, A., Marton, L.F., Bolam, J.P., Brown, P. & Magill, P.J. (2008a) Parkinsonian beta oscillations in the external globus pallidus and their relationship with subthalamic nucleus activity. *J. Neurosci.*, **28**, 14245–14258.
- Mallet, N., Pogossyan, A., Sharott, A., Csicsvari, J., Bolam, J.P., Brown, P. & Magill, P.J. (2008b) Disrupted dopamine transmission and the emergence of exaggerated beta oscillations in subthalamic nucleus and cerebral cortex. *J. Neurosci.*, **28**, 4795–4806.
- Meredith, G.E., Sonsalla, P.K. & Chesselet, M.F. (2008) Animal models of Parkinson's disease progression. *Acta Neuropathol.*, **115**, 385–398.
- Nambu, A. & Llinás, R. (1997) Morphology of globus pallidus neurons: its correlation with electrophysiology in guinea pig brain slices. *J. Comp. Neurol.*, **377**, 85–94.
- Nambu, A., Tokuno, H., Hamada, I., Kita, H., Imanishi, M., Akazawa, T., Ikeuchi, Y. & Hasegawa, N. (2000) Excitatory cortical inputs to pallidal neurons via the subthalamic nucleus in the monkey. *J. Neurophysiol.*, **84**, 289–300.
- Nambu, A., Tachibana, Y., Kaneda, K., Tokuno, H. & Takada, M. (2005) Dynamic model of basal ganglia functions and parkinson's disease. In Bolam, J.P., Ingham, C.A. & Magill, P.J. (Eds), *The Basal Ganglia VIII*. Springer, New York, pp. 307–312.
- Parr-Brownlie, L.C., Poloskey, S.L., Bergstrom, D.A. & Walters, J.R. (2009) Parafascicular thalamic nucleus activity in a rat model of Parkinson's disease. *Exp. Neurol.*, **217**, 269–281.
- Priori, A., Foffani, G., Pesenti, A., Tamma, F., Bianchi, A.M., Pellegrini, M., Locatelli, M., Moxon, K.A. & Villani, R.M. (2004) Rhythm-specific pharmacological modulation of subthalamic activity in Parkinson's disease. *Exp. Neurol.*, **189**, 369–379.
- Rivlin-Etzion, M., Marmor, O., Heimer, G., Raz, A., Nini, A. & Bergman, H. (2006a) Basal ganglia oscillations and pathophysiology of movement disorders. *Curr. Opin. Neurobiol.*, **16**, 629–637.
- Rivlin-Etzion, M., Ritov, Y., Heimer, G., Bergman, H. & Bar-Gad, I. (2006b) Local shuffling of spike trains boosts the accuracy of spike train spectral analysis. *J. Neurophysiol.*, **95**, 3245–3256.
- Sato, F., Lavalée, P., Levesque, M. & Parent, A. (2000) Single-axon tracing study of neurons of the external segment of the globus pallidus in primate. *J. Comp. Neurol.*, **417**, 17–31.
- Schneider, J.S. & Dacko, S. (1991) Relative sparing of the dopaminergic innervation of the globus pallidus in monkeys made hemi-parkinsonian by intracarotid MPTP infusion. *Brain Res.*, **556**, 292–296.
- Sharott, A., Magill, P.J., Harnack, D., Kupsch, A., Meissner, W. & Brown, P. (2005) Dopamine depletion increases the power and coherence of beta-oscillations in the cerebral cortex and subthalamic nucleus of the awake rat. *Eur. J. Neurosci.*, **21**, 1413–1422.
- Shen, K.Z. & Johnson, S.W. (2000) Presynaptic dopamine D2 and muscarinic M3 receptors inhibit excitatory and inhibitory transmission to rat subthalamic neurones *in vitro*. *J. Physiol.*, **525**(Pt 2), 331–341.
- Shen, K.Z. & Johnson, S.W. (2005) Dopamine depletion alters responses to glutamate and GABA in the rat subthalamic nucleus. *Neuroreport*, **16**, 171–174.
- Silberstein, P., Pogossyan, A., Kuhn, A.A., Hotton, G., Tisch, S., Kupsch, A., Dowsey-Limousin, P., Hariz, M.I. & Brown, P. (2005) Cortico-cortical coupling in Parkinson's disease and its modulation by therapy. *Brain*, **128**, 1277–1291.
- Smith, R.D., Zhang, Z., Kurlan, R., McDermott, M. & Gash, D.M. (1993) Developing a stable bilateral model of parkinsonism in rhesus monkeys. *Neuroscience*, **52**, 7–16.

- Smith, Y., Bevan, M.D., Shink, E. & Bolam, J.P. (1998) Microcircuitry of the direct and indirect pathways of the basal ganglia. *Neuroscience*, **86**, 353–387.
- Soares, J., Kliem, M.A., Betarbet, R., Greenamyre, J.T., Yamamoto, B. & Wichmann, T. (2004) Role of external pallidal segment in primate parkinsonism: comparison of the effects of 1-methyl-4-phenyl-1,2,3,6-tetrahydropyridine-induced parkinsonism and lesions of the external pallidal segment. *J. Neurosci.*, **24**, 6417–6426.
- Tachibana, Y., Kita, H., Chiken, S., Takada, M. & Nambu, A. (2008) Motor cortical control of internal pallidal activity through glutamatergic and GABAergic inputs in awake monkeys. *Eur. J. Neurosci.*, **27**, 238–253.
- Watanabe, K., Kita, T. & Kita, H. (2009) Presynaptic actions of D2-like receptors in the rat cortico-striato-globus pallidus disynaptic connection *in vitro*. *J. Neurophysiol.*, **101**, 665–671.
- Wichmann, T. & Soares, J. (2006) Neuronal firing before and after burst discharges in the monkey basal ganglia is predictably patterned in the normal state and altered in parkinsonism. *J. Neurophysiol.*, **95**, 2120–2133.
- Wichmann, T., Bergman, H. & DeLong, M.R. (1994) The primate subthalamic nucleus. III. Changes in motor behavior and neuronal activity in the internal pallidum induced by subthalamic inactivation in the MPTP model of parkinsonism. *J. Neurophysiol.*, **72**, 521–530.
- Williams, D., Tijssen, M., Van Bruggen, G., Bosch, A., Insola, A., Di Lazzaro, V., Mazzone, P., Oliviero, A., Quartarone, A., Speelman, H. & Brown, P. (2002) Dopamine-dependent changes in the functional connectivity between basal ganglia and cerebral cortex in humans. *Brain*, **125**, 1558–1569.
- Yamada, T., McGeer, P.L., Baimbridge, K.G. & McGeer, E.G. (1990) Relative sparing in Parkinson's disease of substantia nigra dopamine neurons containing calbindin-D28K. *Brain Res.*, **526**, 303–307.